Current-induced exchange interactions and effective temperature in localized moment systems

2012 J. Phys.: Condens. Matter 24 116001

(http://iopscience.iop.org/0953-8984/24/11/116001)

IOP Publishing Journal of Physics: Condensed Matter
J. Phys.: Condens. Matter **24** (2012) 116001 (9pp) doi:10.1088/0953-8984/24/11/116001

Current-induced exchange interactions and effective temperature in localized moment systems

Sebastián Díaz[1] **and Álvaro S Núñez**[2]

[1] Department of Physics, University of California, San Diego, La Jolla, CA 92093, USA
[2] Departamento de Física, Facultad de Ciencias Físicas y Matemáticas, Universidad de Chile, Casilla 487-3, Santiago, Chile

E-mail: s1diaz@physics.ucsd.edu and alnunez@dfi.uchile.cl

Received 20 October 2011, in final form 26 December 2011
Published 21 February 2012
Online at stacks.iop.org/JPhysCM/24/116001

Abstract
We study theoretically the spin dynamics of a magnetic dimer serving as a contact between two electrodes. We find that the spin–spin coupling in the dimer can be dramatically modified from its equilibrium value. We show that the interaction can be tuned in such a way that it effectively changes its sign. The calculations show that, for large enough bias, the exchange interaction can even be changed from antiferromagnetic to ferromagnetic. The physical principles behind this result can be used as a new tool to achieve magneto-electric effects in molecular magnet systems.

(Some figures may appear in colour only in the online journal)

1. Introduction

The quest for achieving greater control of the spin degrees of freedom of nanosystems has been a main theme of condensed matter physics and chemistry during the last few decades. The field of spintronics, which depends upon this control in order to create technological devices, has been a major driving force of this topic. When an electric current is driven through a magnetic structure it acquires a spin polarization that is able to substantially modify the coupling between the magnetic elements that conform the structure. Electronic currents, then, can be used to manipulate the magnetic configurations of nanostructures. This feat has been accomplished in several contexts such as current-induced magnetization reversal [1–3], current-driven domain wall motion [4–9] and the spin wave Doppler effect [10–12]. A basic concept behind these experiments is that of spin transfer torque (STT) [13–15]. However, knowledge on the effects of electric currents on the magnetic coupling in the limit of very small magnets is just starting to arise from the experimental work of several groups [16–20]. Interest in these features is linked to the ongoing efforts to create spintronic devices with molecular magnets as constituents, i.e. molecular spintronic devices [21]. The experimental work by Loth *et al* [18] reported the reversal of the atomic spin of an individual Mn adatom located on top of a CuN substrate by means of a spin-polarized tunneling electric current coming from the tip of an STM. The spin polarization was achieved by attaching another Mn atom at the apex of the tip of the STM. The explanation given by these researchers was that inelastic scattering processes of the electrons from the electric current with the Mn adatom excited it to states with higher spin, a mechanism that they called spin-pumping. In this paper we pursue the theoretical principles that dictate the behavior of coupled magnets in the presence of a current. Our approach is based upon the semiclassical treatment of spin fluctuations, which is valid for molecular systems where the magnetic moments are associated with large spin quantum numbers. A full quantum mechanical treatment would complement this work in the cases where such an approximation is not valid. In the case of small magnetic moments, with quantum behavior, such as the case of molecular nanomagnets or magnetic adatoms over metallic surfaces, several non-equilibrium effects [22] have been predicted. Naturally the semiclassical effects to be described here cannot be expected to display the complete phenomenology associated with the quantum

regime. A basic physical picture, nevertheless, can be drawn from the model we use. This physical picture, that we regard as qualitatively accurate, can be used to complement the results of the quantum regime and, as we shall see, shed light on their proper interpretation.

2. Basic model

For definiteness we study a simplified system-plus-reservoir-like model to account for the dynamics of two magnets disposed along an electronic current. Molecular magnet dimers have been synthesized and characterized in several works, and are an adequate platform for the experimental realization of the ideas described here. With this system in mind we will refer to the magnetic moments' degrees of freedom as belonging to a molecular dimer that is located at the junction between two electrodes.

The physical principles we are proposing are unveiled with a very simple model. Indeed, the basic features of the physics we have in mind are displayed by the ideal system depicted in figure 1. This representation is based upon the idea of having a spin dimer connected to electronic leads. The central dimer (hereafter, the system) is described by an s–d exchange-like Hamiltonian. The leads are described by simple free-electron gases, each at equilibrium but with different chemical potentials. The net Hamiltonian of the system is $\mathcal{H} = \mathcal{H}_{\rm R}+\mathcal{H}_{\rm L}+\mathcal{H}_{\rm d}+\mathcal{H}_{\rm Rc}+\mathcal{H}_{\rm Lc}$, where $\mathcal{H}_{\rm R/L} = \sum_{k\sigma}\varepsilon^{\rm R/L}_{k\sigma}c^{\dagger}_{k\sigma}c_{k\sigma}$ is the Hamiltonian describing the physics of the electrons in the reservoirs, where $\varepsilon^{\rm R/L}_{k\sigma}$ stands for the single particle energies,

$$\mathcal{H}_{\rm d} = \sum_a \mathcal{E}(\vec{S}_a) + \epsilon_a n_a - \Delta\vec{S}_a\cdot\vec{s}_a - t_0\sum_\sigma (c^{\dagger}_{1\sigma}c_{2\sigma} + c^{\dagger}_{2\sigma}c_{1\sigma}) \quad (1)$$

is the local Hamiltonian ruling the behavior of the isolated spin dimer. Here, $\mathcal{E}(\vec{S}_a)$ is a single spin Hamiltonian, $n_a = \sum_\sigma c^{\dagger}_{a\sigma}c_{a\sigma}$ is the local electronic number operator, $\vec{S}_a$ is the local moment spin operator, and $\vec{s}_a = \sum_{\sigma\sigma'}\frac{1}{2}\vec{\tau}_{\sigma\sigma'}c^{\dagger}_{a\sigma}c_{a\sigma'}$ is the local electronic spin operator. Notice that in our model the hopping within the molecular dimer is spin independent. Finally, $\mathcal{H}_{\rm Lc} = -t_{\rm L}\sum_\sigma (c^{\dagger}_{\rm L1\sigma}c_{1\sigma}+c^{\dagger}_{1\sigma}c_{\rm L1\sigma})$ and $\mathcal{H}_{\rm Rc} = -t_{\rm R}\sum_\sigma (c^{\dagger}_{\rm R1\sigma}c_{2\sigma}+c^{\dagger}_{2\sigma}c_{\rm R1\sigma})$ are the hopping elements between the system and the leads. Here $c^{\dagger}_{\rm R1\sigma}/c^{\dagger}_{\rm L1\sigma}$ is the electron creation operator at the rightmost/leftmost electron site from the right/left electrode.

The form of the single spin Hamiltonian is quite dependent on the specific chemical nature of the molecular magnet, the simplest non-trivial form is one that accounts for the Zeeman interaction with a fixed external magnetic field **B** and for the magnetocrystalline anisotropy by means of an anisotropic easy-plane:

$$\mathcal{E}(\vec{S}) = -\mathbf{h}\cdot\vec{S} + DS_z^2 - E(S_x^2 - S_y^2), \quad (2)$$

where $\mathbf{h} \equiv g\mu_{\rm B}\mathbf{B}$ ($\mu_{\rm B}$ is the Bohr magneton and g is the g-factor) whereas D and E are magnetocrystalline anisotropic constants defining the easy-axis and in-plane anisotropies, respectively.

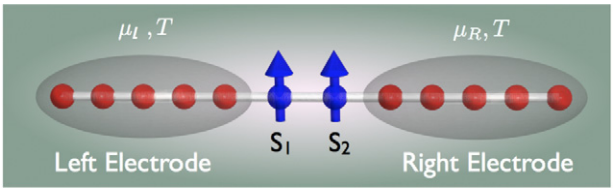

Figure 1. Model system of a spin dimer connected to two leads. The chemical potential of the left lead is $\mu_{\rm L}$ and different from the chemical potential of the right lead $\mu_{\rm R}$. The temperatures T of both leads are for simplicity taken to be equal.

3. Formalism

The basic formalism we will follow is described in [23] for the case of a single spin. Basically we calculate by formal methods the probability density function for the spin orientations, and derive a stochastic differential equation for it [24, 25]. A somewhat simpler calculation, based on linear response theory, was worked out for the single spin case in [26]. Using spin [27] and fermionic [28] coherent states we can build a path integral representation of the probability density $\mathbb{P}[\hat{\mathbf{\Omega}}_1, \hat{\mathbf{\Omega}}_2, t]$. Denoting all the fermionic coherent state labels by Ψ, we can write

$$\mathbb{P}[\hat{\mathbf{\Omega}}_1, \hat{\mathbf{\Omega}}_2, t] = \int_{\mathbf{\Omega}_1(t)=\hat{\mathbf{\Omega}}_1}\int_{\mathbf{\Omega}_2(t)=\hat{\mathbf{\Omega}}_2} \mathcal{D}\mathbf{\Omega}_1\,\mathcal{D}\mathbf{\Omega}_2 \times \int \mathcal{D}^2\Psi\,\delta(|\mathbf{\Omega}_1|^2-1)\delta(|\mathbf{\Omega}_2|^2-1)\,\mathrm{e}^{\frac{\mathrm{i}}{\hbar}\mathcal{S}}. \quad (3)$$

The action of the system consists of three contributions, $\mathcal{S} = \mathcal{S}_\Omega + \mathcal{S}_\Psi + \mathcal{S}_I$. Each term of the action is given explicitly as follows:

$$\mathcal{S}_\Omega = \int_{\mathcal{C}^t}\mathrm{d}t\sum_a\left\{-\hbar S\frac{\mathrm{d}\omega_a}{\mathrm{d}t} - \mathcal{E}[\mathbf{\Omega}_a]\right\}, \quad (4)$$

associated with the isolated spin degrees of freedom ($\mathcal{E}[\mathbf{\Omega}] = -S\mathbf{h}\cdot\mathbf{\Omega} + S^2D\Omega_z^2 - S^2E(\Omega_x^2-\Omega_y^2)$ and ω_a is the spin Berry phase [27]),

$$\mathcal{S}_\Psi = \int_{\mathcal{C}^t}\mathrm{d}t\left\{\mathrm{i}\hbar\sum_\alpha \Psi^*_\alpha(t)\partial_t\Psi_\alpha(t) - \mathcal{H}_\Psi\right\}, \quad (5)$$

associated with the isolated fermionic system, and

$$\mathcal{S}_I = \int_{\mathcal{C}^t}\mathrm{d}t\sum_a S\Delta\,\mathbf{s}_a\cdot\mathbf{\Omega}_a, \quad (6)$$

associated with the interaction between those two. The time integrals are performed over a Keldysh contour $\mathcal{C}^t$ with two branches of time [30]. Integrating the fermion degrees of freedom out of the problem by introducing the average $\langle(\cdots)\rangle \equiv \int\mathcal{D}^2\Psi(\cdots)\mathrm{e}^{\frac{\mathrm{i}}{\hbar}\mathcal{S}_\Psi}$, it can be shown using a cumulant expansion ([32], chapter 6) that up to second order in Δ the probability density becomes $\mathbb{P}[\hat{\mathbf{\Omega}}_1, \hat{\mathbf{\Omega}}_2, t] = \int_{\mathbf{\Omega}_1(t)=\hat{\mathbf{\Omega}}_1}\int_{\mathbf{\Omega}_2(t)=\hat{\mathbf{\Omega}}_2}\mathcal{D}\mathbf{\Omega}_1\mathcal{D}\mathbf{\Omega}_2\,\delta(|\mathbf{\Omega}_1|^2-1)\delta(|\mathbf{\Omega}_2|^2-1)\mathrm{e}^{\frac{\mathrm{i}}{\hbar}\tilde{\mathcal{S}}_\Omega}$. The paths in spin space are now weighted by an effective action, $\tilde{\mathcal{S}}_\Omega = \mathcal{S}_\Omega + \langle\mathcal{S}_I\rangle + \frac{\mathrm{i}}{2\hbar}(\langle\mathcal{S}_I^2\rangle - \langle\mathcal{S}_I\rangle^2)$, which can be

explicitly evaluated as

$$\tilde{\mathcal{S}}_\Omega = \int_{\mathcal{C}^t} \mathrm{d}t \sum_a \left\{ -\hbar S \frac{\mathrm{d}\omega_a}{\mathrm{d}t} - \mathcal{E}[\mathbf{\Omega}_a(t)] + S\Delta \langle \mathbf{s}_a(t) \rangle \cdot \mathbf{\Omega}_a(t) \right\} + \int_{\mathcal{C}^t} \mathrm{d}t \int_{\mathcal{C}^t} \mathrm{d}t' \sum_{abij} \Delta^2 S^2 \mathcal{K}^{ij}_{ab}(t,t') \Omega^i_a(t) \Omega^j_b(t'). \quad (7)$$

The kernel $\mathcal{K}^{ij}_{ab}(t,t')$ is given in terms of spin correlations as follows:

$$\mathcal{K}^{ij}_{ab}(t,t') \equiv \frac{\mathrm{i}}{2\hbar}[\langle \mathcal{T} s^i_a(t) s^j_b(t') \rangle - \langle s^i_a(t) \rangle \langle s^j_b(t') \rangle], \quad (8)$$

where the spin correlations can be evaluated in terms of fermionic averages as $\langle s^i_a(t) \rangle = \sum_{\sigma\sigma'} \frac{1}{2} \tau^i_{\sigma\sigma'} \langle \mathcal{T} \psi_{a\sigma'}(t) \psi^*_{a\sigma}(t) \rangle = 0$ (for our dimer model with spin-independent hopping) and $\langle \mathcal{T} s^i_a(t) s^j_b(t') \rangle = \sum_{\sigma\sigma'\mu\nu} \frac{1}{4} \boldsymbol{\tau}^i_{\sigma\sigma'} \boldsymbol{\tau}^j_{\mu\nu} \langle \mathcal{T} \psi^*_{a\sigma}(t) \psi_{a\sigma'}(t) \psi^*_{b\mu}(t') \psi_{b\nu}(t') \rangle$. Here $\mathcal{T}$ represents the time-ordering operator along the Keldysh contour [30]. The 2-spin correlation function corresponds to a 4-fermion correlation function and can be managed with the aid of Wick's theorem. In terms of the electron Green's functions $G_{a\sigma;b\sigma'}(t,t') \equiv -\mathrm{i} \langle \mathcal{T} \psi_{a\sigma}(t) \psi^*_{b\sigma'}(t') \rangle$ the effective kernel is given by

$$\mathcal{K}^{ij}_{ab}(t,t') = \frac{\mathrm{i}}{8\hbar} \sum_{\sigma\sigma'\mu\nu} \boldsymbol{\tau}^i_{\sigma\sigma'} \boldsymbol{\tau}^j_{\mu\nu} G_{a\sigma';b\mu}(t,t') G_{b\nu;a\sigma}(t',t). \quad (9)$$

The effective dynamics can now be projected into real time [30]. The formal manipulations involved in this process are a straightforward extension of those described in [23]. The final outcome is two coupled Langevin equations for the directions of the local moments in the semiclassical approximation. The zero-mean Gaussian stochastic fields appearing in them, namely $\boldsymbol{\eta}_a(t)$, are interpreted as stochastic magnetic fields. Moreover, it is found that the retarded and advanced components of $\mathcal{K}^{ij}_{ab}(t,t')$ induce effective exchange interactions between $\hat{\mathbf{\Omega}}_1$ and $\hat{\mathbf{\Omega}}_2$, while the Keldysh component rules the correlations of the stochastic magnetic fields: $\langle \boldsymbol{\eta}^i_a(t) \boldsymbol{\eta}^j_b(t') \rangle = -\mathrm{i}\hbar S^2 \Delta^2 \mathcal{K}^{ij(K)}_{ab}(t,t')$. Since the effective kernel was a result of integrating out the electrons, it comes as no surprise that its different components are related to electronic spin correlation functions:

$$\mathcal{K}^{ij(+)}_{ab}(t,t') + \mathcal{K}^{ji(-)}_{ba}(t',t) = \chi^{ij}_{ab}(t-t') \equiv \theta(t-t') \frac{i}{\hbar} \langle [\delta s^i_a(t), \delta s^j_b(t')] \rangle, \quad (10)$$

$$\mathcal{K}^{ij(K)}_{ab}(t,t') = \frac{\mathrm{i}}{\hbar} \frac{1}{2} \langle \{ \delta s^i_a(t), \delta s^j_b(t') \} \rangle. \quad (11)$$

Above we introduced the spin fluctuation operator $\delta s^i_a(t) \equiv s^i_a(t) - \langle s^i_a(t) \rangle$. The evaluation of these correlation functions is cumbersome but straightforward. A brief account of it is given in the appendix. In the low energy limit, the Langevin equations take the form

$$\begin{aligned} \hbar S \frac{\mathrm{d}\hat{\mathbf{\Omega}}_1}{\mathrm{d}t} &= \hat{\mathbf{\Omega}}_1 \times \left[-\frac{\partial}{\partial \hat{\mathbf{\Omega}}_1} (\mathcal{E}[\hat{\mathbf{\Omega}}_1] - S^2 \mathcal{J}_{12} \hat{\mathbf{\Omega}}_1 \cdot \hat{\mathbf{\Omega}}_2) + \boldsymbol{\eta}_1 - \hbar S^2 \sum_a \alpha_{1a} \frac{\mathrm{d}\hat{\mathbf{\Omega}}_a}{\mathrm{d}t} \right], \\ \hbar S \frac{\mathrm{d}\hat{\mathbf{\Omega}}_2}{\mathrm{d}t} &= \hat{\mathbf{\Omega}}_2 \times \left[-\frac{\partial}{\partial \hat{\mathbf{\Omega}}_2} (\mathcal{E}[\hat{\mathbf{\Omega}}_2] - S^2 \mathcal{J}_{21} \hat{\mathbf{\Omega}}_1 \cdot \hat{\mathbf{\Omega}}_2) + \boldsymbol{\eta}_2 - \hbar S^2 \sum_a \alpha_{2a} \frac{\mathrm{d}\hat{\mathbf{\Omega}}_a}{\mathrm{d}t} \right]. \end{aligned} \quad (12)$$

The effective exchange coupling constants are given by

$$\mathcal{J}_{ab} \equiv \tfrac{1}{3} \Delta^2 \hbar \sum_i \chi^{ii}_{ab}(\epsilon = 0) \quad (13)$$

and the damping coefficients are

$$\alpha_{ab} \equiv -\frac{\mathrm{i}}{3} \hbar \Delta^2 \sum_i \left[\frac{\mathrm{d}\chi^{ii}_{ab}}{\mathrm{d}\epsilon} \right]_{\epsilon=0}. \quad (14)$$

Furthermore, in the low energy limit the electron dynamics is faster than that of the local moments which allows us to make the approximation $\langle \boldsymbol{\eta}^i_a(t) \boldsymbol{\eta}^j_b(t') \rangle = \delta(t-t')[-\mathrm{i}\hbar^2 S^2 \Delta^2 \mathcal{K}^{ij(K)}_{ab}(\epsilon \to 0)]$. In the subsequent developments, it proves useful to define c_{ab} as

$$\mathcal{K}^{ij(K)}_{ab}(\epsilon \to 0) = \delta^{ij} \frac{\mathrm{i}}{\hbar} c_{ab}. \quad (15)$$

Expressions for these three coefficients in terms of the Green's functions of the integrated out electrons can be found by simple, though lengthy, manipulations. These coefficients have the simplified expressions described in the appendix. We remark that these coefficients are functions of the electrode temperature T and chemical potentials μ_L, μ_R through the electron Green's functions. Writing $\mu_\mathrm{L} = \mu_\mathrm{F} + \frac{eV}{2}$, $\mu_\mathrm{R} = \mu_\mathrm{F} - \frac{eV}{2}$ we see how they also depend on the bias voltage V across the spin dimer. μ_F is proportional to the so-called gate voltage. In what follows we will use $\mu_{1/2} \equiv \mu_{\mathrm{L/R}}$. The steady-state probability density can be easily calculated for the case when one of the localized spins is kept fixed. This case is of interest because this situation is realized in experiments. Before we dwell on an application of the formalism discussed above, we find it convenient to discuss one feature of the equations that has no simple analogy in the common treatments of magnetization dynamics. If we define the effective energy functional

$$\mathcal{E}_\mathrm{eff}[\hat{\mathbf{\Omega}}_1, \hat{\mathbf{\Omega}}_2] = \mathcal{E}[\hat{\mathbf{\Omega}}_1] - S^2 \mathcal{J}_{12} \hat{\mathbf{\Omega}}_1 \cdot \hat{\mathbf{\Omega}}_2 + \mathcal{E}[\hat{\mathbf{\Omega}}_2] - S^2 \mathcal{J}_{21} \hat{\mathbf{\Omega}}_2 \cdot \hat{\mathbf{\Omega}}_1 \quad (16)$$

we can find its time derivative through the use of equations (12):

$$\frac{\mathrm{d}}{\mathrm{d}t} \mathcal{E}_\mathrm{eff}[\hat{\mathbf{\Omega}}_1, \hat{\mathbf{\Omega}}_2] = [\boldsymbol{\eta}_1 - S^2 \mathcal{J}_{21} \hat{\mathbf{\Omega}}_2] \cdot \frac{\mathrm{d}\hat{\mathbf{\Omega}}_1}{\mathrm{d}t} + [\boldsymbol{\eta}_2 - S^2 \mathcal{J}_{12} \hat{\mathbf{\Omega}}_1] \cdot \frac{\mathrm{d}\hat{\mathbf{\Omega}}_2}{\mathrm{d}t}$$

$$-\hbar S^2\left[\alpha_{11}\left(\frac{\mathrm{d}\hat{\boldsymbol{\Omega}}_1}{\mathrm{d}t}\right)^2+\alpha_{22}\left(\frac{\mathrm{d}\hat{\boldsymbol{\Omega}}_2}{\mathrm{d}t}\right)^2 + (\alpha_{12}+\alpha_{21})\frac{\mathrm{d}\hat{\boldsymbol{\Omega}}_1}{\mathrm{d}t}\cdot\frac{\mathrm{d}\hat{\boldsymbol{\Omega}}_2}{\mathrm{d}t}\right] \tag{17}$$

in addition to the standard contributions we have a crossed term that contributes to the dissipation. The time derivative of one of the moments induces damping torques in the other in a fashion similar to the Gilbert damping phenomenology. The effect of the damping mechanisms will be to take energy away from the spins as long as the matrix α is positive-definite.

4. Results with one spin fixed

In an experiment involving an STM prepared to perform spin-polarized measurements, the tip has a more or less fixed magnetization. Placing the tip above a localized spin lying on the surface of some substrate and then applying a bias voltage to generate a current is the experimental realization of our theoretical model[3]. To obtain a clearer picture of the physics that is embodied in the equations above let us suppose that the localized spin at site 1 is fixed along the direction $\hat{\mathbf{n}}$ and only $\hat{\boldsymbol{\Omega}}_2$ is free to move. The description of the system is then simplified and from the two coupled Langevin equations we are left with only one that determines the dynamics of the localized spin at site 2. Since now $\hat{\boldsymbol{\Omega}}_1 = \hat{\mathbf{n}}$ we can drop the subscript from $\hat{\boldsymbol{\Omega}}_2$ and $\boldsymbol{\eta}_2$ without causing any confusion. The resulting Langevin equation corresponds to the dynamics of a single fluctuating moment and yields the following stationary probability density that also depends on V:

$$\mathbb{P}[\hat{\boldsymbol{\Omega}}, V] = N\exp\left[-\frac{2\alpha_{22}(V)}{\Delta^2 c_{22}(V)}(\mathcal{E}[\hat{\boldsymbol{\Omega}}] - S^2\mathcal{J}_{21}(V)\hat{\boldsymbol{\Omega}}\cdot\hat{\mathbf{n}})\right], \tag{18}$$

with N a normalization constant. The similarity of $\mathbb{P}[\hat{\boldsymbol{\Omega}}, V]$ and the probability density in the canonical ensemble from statistical mechanics motivates the definition of an effective temperature,

$$k_{\mathrm{B}}T_{\mathrm{eff}} = \frac{\Delta^2 c_{22}(V)}{2\alpha_{22}(V)}, \tag{19}$$

which is a function of both the temperature of the electrodes and the voltage drop across them.

The physics of the localized spin at site 2 is determined by the Gilbert damping α_{22}, the correlation strength c_{22} and the effective exchange interaction $\mathcal{J}_{21}$. We numerically calculated them as functions of μ_{F} and V for the electronic parameters $\epsilon_1 = 0$ meV $= \epsilon_2$, $J = 100$ meV, $t_0 = 2$ meV, $t_{\mathrm{L}} = 10$ meV $= t_{\mathrm{R}}$. In all the calculations reported here we took $T = 0$ K, which is justified when $k_{\mathrm{B}}T \ll |eV|$, a condition usually achieved in experiments. The relaxation of this condition to include temperature effects is straightforward

[3] In such a situation an asymmetric parametrization of $\mu_{1/2}$ emphasizing the asymmetry between the two leads is customary. In that case it is a simple matter to change the results below by an arithmetic transformation.

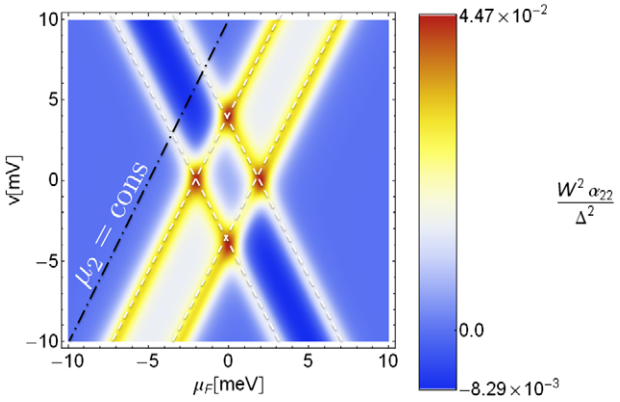

Figure 2. Gilbert damping α_{22}. The local maxima occur along the dashed lines $\mu_1 = \pm t_0$ and $\mu_2 = \pm t_0$, α_{22}, being larger on $\mu_2 = \pm t_0$. The global maxima are attained at the four intersection points of the lines of local maxima. The Gilbert damping describes energy injection, i.e. $\alpha_{22} < 0$, in the region determined by $|\mu_1| < t_0$ and $|\mu_2| > t_0$.

in our calculations. To adimensionalize the coefficients a characteristic energy value from the electrodes, denoted by W, was used. The imaginary part of the selfenergy due to the electrodes is related to the density of states (DOS) of the electrodes at the point of contact with the spin dimer. Usually this function is practically constant near the Fermi level where the electronic processes involved occur. Then we chose W as the value at the Fermi level of the imaginary part in the energy representation of the selfenergy. The specific expression is $W \equiv |\hbar\,\mathrm{Im}\,\Sigma^{(+)}_{1/2}(\epsilon = 0)| = \frac{t^2_{\mathrm{L/R}}}{J}$, which is equal to 1 meV for the above electronic parameters.

Key to the interpretation of our results is the DOS of the two electronic sites of the spin dimer renormalized by the electrodes. In the absence of electrodes, the eigenstates of the Hamiltonian describing the two electronic sites are the well-known bonding and antibonding states. The DOS of this isolated system has two pronounced peaks at their corresponding eigenenergies which for the chosen parameters are $\pm t_0$. Coupling to the electrodes changes the DOS broadening the peaks at these eigenenergies.

The calculated density plots for the three coefficients exhibit a cross-like pattern with a diamond-like quadrilateral at its center. The lines defining the crosses are determined by the equations $\mu_1 = \pm t_0$ and $\mu_2 = \pm t_0$, which correspond to the case when the chemical potentials are just at the center of either of the two maxima of the DOS. This means that electrode i tries to enforce a nearly singly occupied (for $\mu_i = -t_0$) or a nearly triply occupied (for $\mu_i = t_0$) electronic system.

The density plot in figure 2, corresponding to the Gilbert damping α_{22}, shows that its local maxima occur on the lines that define the aforementioned cross-like pattern. It is also observed that α_{22} is larger on the line of local maxima $\mu_2 = \pm t_0$ than on the line $\mu_1 = \pm t_0$, hinting that when $\mu_2 \approx \pm t_0$ the energy of the localized spin at site 2 is mostly dissipated to the closest electrode. The global maxima of α_{22} are attained when both chemical potentials are at any of the maxima of the electronic DOS, i.e., at the four points where the dashed

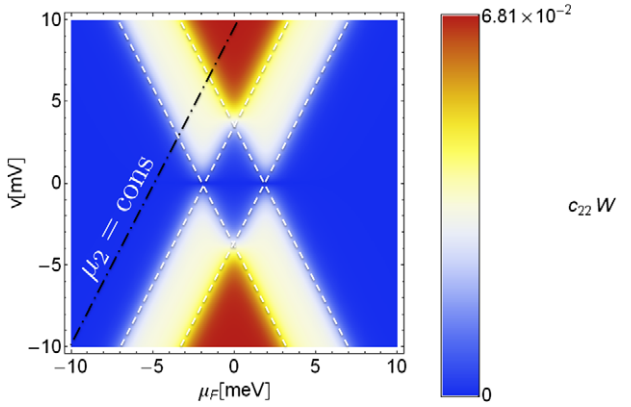

Figure 3. The stochastic magnetic field correlation strength c_{22}. It is observed that c_{22} increases in a step-like form when the chemical potentials from each electrode try to occupy the electronic system with slightly more than one or three electrons. Both situations correspond to configurations where the electronic system allows charge fluctuations. This behavior is similar to the shot noise [29] measured in mesoscopic conductors.

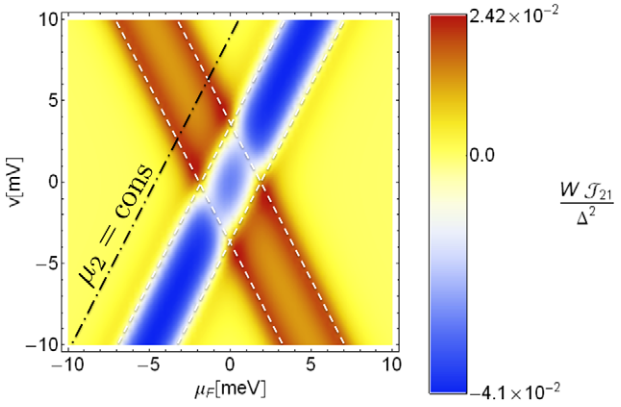

Figure 4. The effective exchange interaction $\mathcal{J}_{21}$. The antiferromagnetic configuration ($\mathcal{J}_{21} < 0$) is attained in the region determined approximately by $|\mu_1| > t_0$ and $|\mu_2| < t_0$, while the rest of the (μ_F, V) plane allows a ferromagnetic configuration ($\mathcal{J}_{21} > 0$). The local maxima of $\mathcal{J}_{21}$ (ferromagnetic) are attained along the lines $\mu_1 = \pm t_0$ and the global maxima are located near the four intersection points of the dashed lines $\mu_1 = \pm t_0$ and $\mu_2 = \pm t_0$. The global minima of $\mathcal{J}_{21}$ (antiferromagnetic) are attained along the line $\mu_2 = 0$.

lines of the local maxima intersect. The region where instead of dissipation the Gilbert damping describes an injection of energy can be precisely determined from this density plot. It turns out that $\alpha_{22} < 0$ when $|\mu_1| < t_0$ and $|\mu_2| > t_0$. We interpret this result by recalling that the entire spin dimer is losing energy; however, nothing prevents the other localized spin, the fixed one in this case, from giving some energy to the one at site 2 if the net energy of the spin dimer has not increased.

The stochastic magnetic field correlation strength c_{22}, depicted in figure 3, is always zero at $V = 0$. This behavior can be justified by recalling that these correlations are originated by the electronic spin fluctuations. At zero temperature, in the absence of electric currents and within the approximation of slow dynamics for the localized spins, the electronic spin fluctuations and therefore c_{22} vanish. For nonzero bias voltage c_{22} increases its value in a step-like form when the chemical potentials from any of the two electrodes are increased and just start to allow more than one or more than three electrons in the system. Both situations can be understood by noting that when the electronic system has slightly more than one/three electrons the remnant of the bonding/antibonding state is not fully occupied and allows charge fluctuations. This behavior is similar to the shot noise [29] measured in mesoscopic conductors; systems which are also described by a discrete set of energy levels through which electronic conduction occurs.

The last density plot, figure 4, shows the behavior of the effective exchange interaction $\mathcal{J}_{21}$. Interesting findings are that $\mathcal{J}_{21}$ can be positive or negative at zero bias voltage and that it can change its sign even more than once while sweeping V at fixed gate voltage. Again, these features depend on the center of the bias voltage window with respect to the electronic DOS. The antiferromagnetic configuration ($\mathcal{J}_{21} < 0$) is attained in the region determined approximately by $|\mu_1| > t_0$ and $|\mu_2| < t_0$, while the rest of the (μ_F, V) plane allows a ferromagnetic configuration ($\mathcal{J}_{21} > 0$). The more pronounced features of the density plot of $\mathcal{J}_{21}$ are observed near the lines that determine the cross-like pattern. The local maxima of $\mathcal{J}_{21}$ (ferromagnetic) are attained along the lines $\mu_1 = \pm t_0$ and the global maxima are located near the four intersection points of the lines $\mu_1 = \pm t_0$ and $\mu_2 = \pm t_0$. The global minima of $\mathcal{J}_{21}$ (antiferromagnetic) are attained along the line $\mu_2 = 0$. We can understand such behavior by analyzing it in the zero bias regime. As can be appreciated by studying figure 4, even in the case of zero bias, the exchange coupling has a non-monotonic behavior as a function of the equilibrium chemical potential. There is a transition between a regime of double exchange into antiferromagnetic exchange as the number of electrons changes from an even to an odd number. The transition point in the equilibrium regime is directly $\mu_2 = \pm t_0$. This point is a zero and not a local maximum of the exchange constant. The basic underlying process behind the change of sign in the exchange coupling is the excitation from bonding to antibonding states driven by the bias. The possibility of such excitation leads to electron occupations that fluctuate wildly between positive and negative values. Moreover, the variation of the electronic hoppings and on-site energies can add even more tunable possibilities that could enable an engineered effective exchange coupling. To understand these results we must keep in mind that the electronic energies are located at $\pm t_0$ (see figure 5(d)) but are spread by the excursions into the leads. Such spreading reduces the voltage necessary to excite the electronic cloud into the antibonding configuration, changing the effective exchange.

5. Discussion

The experimental work by Loth *et al* [18] reported the reversal of the atomic spin of an individual Mn adatom located on top of a CuN substrate by means of a spin-polarized tunneling electric current coming from the tip of an STM. The spin

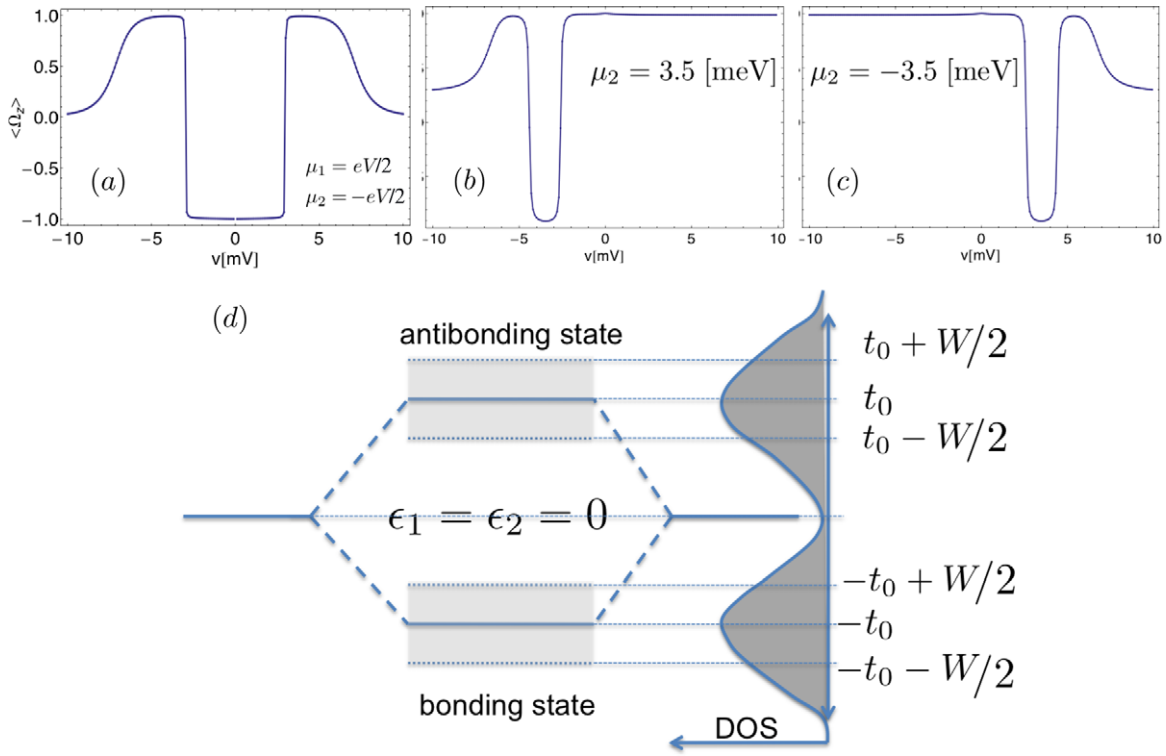

Figure 5. $\langle\Omega_z\rangle$ current-driven reversal. (a) Plot of the z component of the free localized spin of the spin dimer that represents the atomic spin of the Mn adatom. The fixed localized spin is pointing in the $\hat{\mathbf{k}}$ direction. The plot was calculated for $\mu_F = 0$ meV, $T = 0$ K, $S = 5/2$, $g = 1.9$, $B = 7$ T, $D = -0.39$ meV, $\Delta = 20$ meV, and $E = 0.07$ meV. It shows that at $V = 0$ the spin dimer has an antiferromagnetic configuration. Upon increasing or decreasing the bias voltage, approximately near ± 3 mV, a reversal occurs toward a ferromagnetic configuration. (b) Plot analogous to (a) but fixing the chemical potential of one lead ($\mu_2 = 3.5$ (meV)) while tuning the other with the bias voltage ($\mu_1 = \mu_2 + eV$). (c) Similar to (b) with $\mu_2 = -3.5$ (meV). (d) Energies of the electronic states in the isolated dimer. The bonding and antibonding states are respectively spread by the coupling to the leads. Cartoon of the density of states of the isolated dimer illustrating the spreading of the electronic states.

polarization was achieved by attaching another Mn atom at the apex of the tip of the STM. The explanation given by these researchers was that inelastic scattering processes of the electrons from the electric current with the Mn adatom excited it to states with higher spin, a mechanism that was coined as spin-pumping.

The theoretical model that we have developed allows us to give a semiclassical explanation of this reported reversal phenomenon. First we should note that the basic physics describing the dynamics of electrons and localized moments has been treated in several places with model Kondo-like Hamiltonians [33, 34]. The atomic spins of the Mn atoms are modeled by the localized spins of our spin dimer and the tunneling electric current is incorporated by the bias voltage between the electrodes. Considering that what must be described in this experiment is the relative positions of the atomic spins of the Mn atoms, we regarded the localized spin representing the atomic spin from the Mn atom at the tip as fixed. Using the electronic parameter values used above and the parameters reported in [18] ($S = 5/2$, $g = 1.9$, $B = 7$ T, $D = -0.39$ meV, $\Delta = 20$ meV and $E = 0.07$ meV) we determined the steady-state probability density for the direction of the free localized spin for an arbitrary bias voltage V (18). Then, we numerically calculated the z-component, $\langle\Omega_z\rangle$, of the free localized spin that represents the atomic spin of the Mn adatom, as a function of the bias voltage (figure 5).

It is observed that at $V = 0$ mV and in its neighborhood, $\langle\Omega_z\rangle$ is negative which means that the localized spins tend to be aligned antiferromagnetically. As the bias voltage decreases/increases this situation is maintained; however, approximately near $V = \pm 3$ mV, $\langle\Omega_z\rangle$ changes its sign and the localized spins tend to be ferromagnetically aligned. This result is due to the excitation, when the bias is large enough, of the antibonding electronic states. The effects of this contribution alter the effective exchange interaction $\mathcal{J}_{21}$, the correlation strength c_{22} and the Gilbert damping α_{22}. These three coefficients determine the steady-state probability density for the direction of the free localized spin, as can be seen in (18).

The exact mechanisms involved in the reversal can be further investigated by looking at the probability density more closely. Plots like those shown in figure 6 are particularly enlightening. Study of the evolution and reordering of the probability density on the sphere as the bias voltage changes could shed light on the microscopic details and the role of the magnetic anisotropies, modeled by D and E, that lead to the reversal. Before we finish we will discuss the applicability of spin transfer physics. Truncation of the action to terms proportional to second order in Δ makes it inviable to attach to STTs any role in the reversal process just described. This can be checked easily as follows. In the geometry described

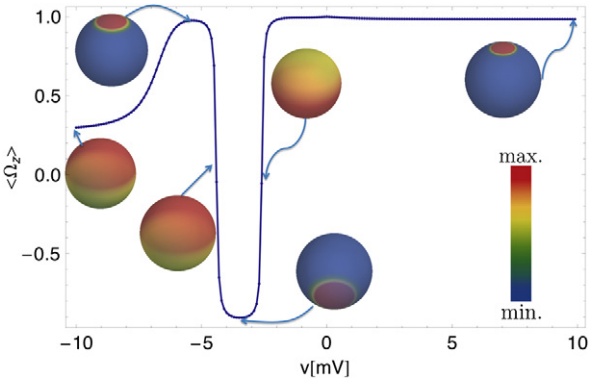

Figure 6. The probability density for the direction of the free localized spin. The parameters used are the same as those in figure 5(b). The probability density plots at $V = -10$, -5, -4.43, -3.5, -2.61 and 10 mV are displayed. The color code for the probability density is given in the inset. At $V = -3.5$ mV the plot shows a higher probability density near the 'south pole' that gives a negative value for $\langle\Omega_z\rangle$, while the plots at $V = -5$, 10 mV have a higher probability density near the 'north pole' which gives a positive $\langle\Omega_z\rangle$. These plots represent an antiferromagnetic and a ferromagnetic configuration, respectively, as explained in the text. The plots at $V = -4.43$ and -2.61 mV that exhibit a more complex distribution of the probability density are characteristic of the reversal of $\langle\Omega_z\rangle$.

above the generic form of the spin transfer torque is

$$\delta\vec{\boldsymbol{\tau}}_{\rm STT} \propto (\hat{\boldsymbol{\Omega}}_1 \times \hat{\boldsymbol{\Omega}}_2) \times \hat{\boldsymbol{\Omega}}_2; \tag{20}$$

this term clearly breaks time reversal symmetry leading to a dissipative torque. On the other hand the reversal we are arguing for is driven by the form

$$\delta\vec{\boldsymbol{\tau}}_{\rm neq-exchange} \propto (\hat{\boldsymbol{\Omega}}_1 \times \hat{\boldsymbol{\Omega}}_2), \tag{21}$$

evidently a time reversal invariant contribution. This form has been found in the literature on spin torque [35]. We present an analysis of its dynamical consequences in the regime where it is the dominant term.

In conclusion we have discussed a set of phenomena expected to affect the coupling between small magnets under current. We have illustrated, using a simple toy model, that the non-equilibrium electrons are able to severely alter the exchange constants of the equilibrium situation. Finally, we have used the ideas above to discuss and explain the spin dynamics in the experimental setting described in [18].

Acknowledgments

This work was partially funded by Proyecto Fondecyt numbers 11070008 and 1110271, Proyecto Basal FB0807-CEDENNA, and by Núcleo Científico Milenio P10-061-F.

Appendix. Electron correlation calculations

The interactions between the localized spins of the spin dimer are mediated by the electronic environment and are determined by an integral kernel. This kernel also has a dependence on the electronic sites of the spin dimer

$$\mathcal{K}^{ij}_{ab}(t,t') \equiv \frac{\mathrm{i}}{2\hbar}[\langle \mathcal{T} s^i_a(t) s^j_b(t')\rangle - \langle s^i_a(t)\rangle\langle s^j_b(t')\rangle]. \tag{A.1}$$

The total electronic spin at the electronic sites appears in this definition. Using the Grassman fields corresponding to site a, the ith component of the total electronic spin at site a can be written as

$$s^i_a(t) = \sum_{\sigma,\sigma'} \tfrac{1}{2}\psi^*_{a\sigma}(t)\boldsymbol{\tau}^i_{\sigma\sigma'}\psi_{a\sigma'}(t). \tag{A.2}$$

This integral kernel can also be decomposed into its lesser and greater components

$$\mathcal{K}^{ij}_{ab}(t,t') = \theta(t-t')\mathcal{K}^{ij>}_{ab}(t,t') + \theta(t'-t)\mathcal{K}^{ij<}_{ab}(t,t'). \tag{A.3}$$

Moreover, the retarded, advanced and Keldysh components are given by

$$\mathcal{K}^{ij(\pm)}_{ab}(t,t') = \pm\theta[\pm(t-t')][\mathcal{K}^{ij>}_{ab}(t,t') - \mathcal{K}^{ij<}_{ab}(t,t')], \tag{A.4}$$

$$\mathcal{K}^{ij(K)}_{ab}(t,t') = \mathcal{K}^{ij>}_{ab}(t,t') + \mathcal{K}^{ij<}_{ab}(t,t'). \tag{A.5}$$

We shall now express the various components of $\mathcal{K}^{ij}_{ab}(t,t')$ first in terms of electronic spin correlations and secondly in terms of the electronic Green's functions. Regarding the first of the two aforementioned intentions, it can be shown that

$$\mathcal{K}^{ij}_{ab}(t,t') = \frac{\mathrm{i}}{2\hbar}\theta(t-t')\langle\delta s^i_a(t)\delta s^j_b(t')\rangle + \frac{\mathrm{i}}{2\hbar}\theta(t'-t)\langle\delta s^j_b(t')\delta s^i_a(t)\rangle. \tag{A.6}$$

To get this result, the definition of the time-ordering operator $\mathcal{T}$ was used together with the property that for any two operators A and B it holds that $\langle AB\rangle - \langle A\rangle\langle B\rangle = \langle\delta A\delta B\rangle$, with $\delta A \equiv A - \langle A\rangle$ being the fluctuation of A. For the present case, the ith component of the total electronic spin fluctuation at site a is defined as $\delta s^i_a(t) \equiv s^i_a(t) - \langle s^i_a(t)\rangle$. The lesser and greater components are then expressed as the following correlations of electronic spin fluctuations:

$$\mathcal{K}^{ij>}_{ab}(t,t') = \frac{\mathrm{i}}{2\hbar}\langle\delta s^i_a(t)\delta s^j_b(t')\rangle, \tag{A.7}$$

$$\mathcal{K}^{ij<}_{ab}(t,t') = \frac{\mathrm{i}}{2\hbar}\langle\delta s^j_b(t')\delta s^i_a(t)\rangle. \tag{A.8}$$

Some trivial index gymnastics allows one to prove that $\mathcal{K}^{ji\gtrless}_{ba}(t',t) = \mathcal{K}^{ij\lessgtr}_{ab}(t,t')$. With this last result we find that the retarded and advanced components of $\mathcal{K}^{ij}_{ab}(t,t')$ are directly related to the magnetic susceptibility,

$$\mathcal{K}^{ij(+)}_{ab}(t,t') = \mathcal{K}^{ji(-)}_{ba}(t',t) = \tfrac{1}{2}\theta(t-t')\frac{\mathrm{i}}{\hbar}\langle[\delta s^i_a(t), \delta s^j_b(t')]\rangle = \tfrac{1}{2}\chi^{ij}_{ab}(t-t'), \tag{A.9}$$

and the Keldysh component to the symmetrized correlation of the electronic spin fluctuations,

$$\mathcal{K}^{ij(K)}_{ab}(t,t') = \frac{\mathrm{i}}{\hbar}\frac{1}{2}\langle\{\delta s^i_a(t), \delta s^j_b(t')\}\rangle. \tag{A.10}$$

Using the Green's function decomposition, $G_{a\sigma;b\sigma'}(t,t') = \theta(t-t')G^{>}_{a\sigma;b\sigma'}(t,t') + \theta(t'-t)G^{<}_{a\sigma;b\sigma'}(t,t')$, and the Heaviside function properties, $\theta(t)^2 = \theta(t)$ and $\theta(t)\theta(-t) = 0$, we finally find

$$\mathcal{K}^{ij>}_{ab}(t,t') = \frac{\mathrm{i}}{8\hbar}\sum_{\sigma\sigma'\mu\nu}\boldsymbol{\tau}^{i}_{\sigma\sigma'}\boldsymbol{\tau}^{j}_{\mu\nu}G^{>}_{a\sigma';b\mu}(t,t') \times G^{<}_{bv;a\sigma}(t',t), \tag{A.11}$$

$$\mathcal{K}^{ij<}_{ab}(t,t') = \frac{\mathrm{i}}{8\hbar}\sum_{\sigma\sigma'\mu\nu}\boldsymbol{\tau}^{i}_{\sigma\sigma'}\boldsymbol{\tau}^{j}_{\mu\nu}G^{<}_{a\sigma';b\mu}(t,t') \times G^{>}_{bv;a\sigma}(t',t). \tag{A.12}$$

Since the hopping in the spin dimer is spin independent the electronic Green's functions are diagonal in spin space, $G_{a\sigma;b\sigma'}(t,t') = (\frac{1}{2}\sum_{\rho}G_{a\rho;b\rho}(t,t'))\delta_{\sigma\sigma'} \equiv G_{ab}(t,t')\delta_{\sigma\sigma'}$, and then the lesser and greater components of the kernel take the simple form

$$\mathcal{K}^{ij\gtrless}_{ab}(t,t') = \frac{\mathrm{i}}{4\hbar}\delta^{ij}G^{\gtrless}_{ab}(t,t')G^{\lessgtr}_{ba}(t',t). \tag{A.13}$$

Anti-Fourier transforming the Green's functions components, the following integral representation is obtained:

$$\mathcal{K}^{ij\gtrless}_{ab}(t,t') = \frac{\mathrm{i}}{4\hbar}\delta^{ij}\int\frac{\mathrm{d}\epsilon'}{2\pi}\int\frac{\mathrm{d}\epsilon''}{2\pi}\,\mathrm{e}^{\frac{\mathrm{i}}{\hbar}(\epsilon''-\epsilon')(t-t')} \times G^{\gtrless}_{ab}(\epsilon')G^{\lessgtr}_{ba}(\epsilon''). \tag{A.14}$$

Using this integral representation, the magnetic susceptibility and the Keldysh component are written in energy representation as

$$\chi^{ij}_{ab}(\epsilon) = -\frac{1}{2\hbar}\delta^{ij}\int\frac{\mathrm{d}\epsilon'}{2\pi}\int\frac{\mathrm{d}\epsilon''}{2\pi}\frac{\mathcal{G}_{ab-}(\epsilon',\epsilon'')}{\epsilon+\epsilon''-\epsilon'+\mathrm{i}\eta}, \tag{A.15}$$

$$\mathcal{K}^{ij(K)}_{ab}(\epsilon) = \frac{1}{4\hbar}\delta^{ij}(2\pi\mathrm{i})\int\frac{\mathrm{d}\epsilon'}{2\pi} \times \int\frac{\mathrm{d}\epsilon''}{2\pi}\delta(\epsilon+\epsilon''-\epsilon')\mathcal{G}_{ab+}(\epsilon',\epsilon''), \tag{A.16}$$

where $\mathcal{G}_{ab\pm}(\epsilon',\epsilon'') \equiv G^{>}_{ab}(\epsilon')G^{<}_{ba}(\epsilon'') \pm G^{<}_{ab}(\epsilon')G^{>}_{ba}(\epsilon'')$. Finally, from the definitions (13)–(15), the effective exchange couplings, the Gilbert damping coefficients and the strengths of the stochastic magnetic field correlations are respectively given by

$$\mathcal{J}_{ab} = -\frac{1}{2}\Delta^2\int\frac{\mathrm{d}\epsilon'}{2\pi}\int\frac{\mathrm{d}\epsilon''}{2\pi}\frac{\mathcal{G}_{ab-}(\epsilon',\epsilon'')}{\epsilon''-\epsilon'+\mathrm{i}\eta}, \tag{A.17}$$

$$\alpha_{ab} = \frac{\mathrm{i}}{2}\Delta^2\int\frac{\mathrm{d}\epsilon'}{2\pi}\int\frac{\mathrm{d}\epsilon''}{2\pi}\mathcal{G}_{ab-}(\epsilon',\epsilon'') \times \frac{\partial}{\partial\epsilon''}\left[\frac{1}{\epsilon''-\epsilon'+\mathrm{i}\eta}\right], \tag{A.18}$$

$$c_{ab} = \tfrac{1}{4}\int\frac{\mathrm{d}\epsilon'}{2\pi}\mathcal{G}_{ab+}(\epsilon',\epsilon'). \tag{A.19}$$

For the special case in which the localized spin at the electronic site 1 of the spin dimer is kept fixed, only $\mathcal{J}_{21}$, α_{22} and c_{22} are of importance to describe the spin dimer. These coefficients have the simplified expressions

$$\mathcal{J}_{21} = -\frac{1}{2}\Delta^2\int\frac{\mathrm{d}\epsilon'}{2\pi} \times \int\frac{\mathrm{d}\epsilon''}{2\pi}\frac{G^{>}_{21}(\epsilon')G^{<}_{12}(\epsilon'') - G^{<}_{21}(\epsilon')G^{>}_{12}(\epsilon'')}{\epsilon''-\epsilon'+\mathrm{i}\eta}, \tag{A.20}$$

$$\alpha_{22} = -\frac{1}{4}\Delta^2\int\frac{\mathrm{d}\epsilon'}{2\pi} \times \left[G^{>}_{22}(\epsilon')\frac{\partial}{\partial\epsilon'}G^{<}_{22}(\epsilon') - G^{<}_{22}(\epsilon')\frac{\partial}{\partial\epsilon'}G^{>}_{22}(\epsilon')\right], \tag{A.21}$$

$$c_{22} = \frac{1}{2}\int\frac{\mathrm{d}\epsilon'}{2\pi}G^{>}_{22}(\epsilon')G^{<}_{22}(\epsilon'). \tag{A.22}$$

Following the standard procedure explained in detail in [31], the lesser and greater components of the electron Green's functions are calculated as

$$G^{>}_{ab}(\epsilon) = -\mathrm{i}\sum_{c=1}^{2}[1-n_{\mathrm{F}}(\epsilon-\mu_c)]A_{c;ab}(\epsilon), \tag{A.23}$$

$$G^{<}_{ab}(\epsilon) = \mathrm{i}\sum_{c=1}^{2}n_{\mathrm{F}}(\epsilon-\mu_c)A_{c;ab}(\epsilon), \tag{A.24}$$

with $n_{\mathrm{F}}(\epsilon) = \{\exp[\frac{\epsilon}{k_{\mathrm{B}}T}]+1\}^{-1}$ the Fermi–Dirac distribution function, $\mu_{1/2} \equiv \mu_{\mathrm{L/R}}$ and the spectral functions given by

$$A_{c;ab}(\epsilon) = G^{(+)}_{ac}(\epsilon)\,\mathrm{Im}[-2\hbar\Sigma^{(+)}_{c}(\epsilon)]G^{(-)}_{cb}(\epsilon). \tag{A.25}$$

The retarded and advanced Green's functions are

$$G^{(\pm)}_{11}(\epsilon) = \frac{g^{(\pm)}_{2}(\epsilon)}{g^{(\pm)}_{1}(\epsilon)g^{(\pm)}_{2}(\epsilon)-t_0^2}, \tag{A.26}$$

$$G^{(\pm)}_{12}(\epsilon) = G^{(\pm)}_{21}(\epsilon) = \frac{t_0}{g^{(\pm)}_{1}(\epsilon)g^{(\pm)}_{2}(\epsilon)-t_0^2}, \tag{A.27}$$

$$G^{(\pm)}_{22}(\epsilon) = \frac{g^{(\pm)}_{1}(\epsilon)}{g^{(\pm)}_{1}(\epsilon)g^{(\pm)}_{2}(\epsilon)-t_0^2}, \tag{A.28}$$

where $g^{(\pm)}_{a}(\epsilon) \equiv \epsilon - \epsilon_a - \hbar\Sigma^{(\pm)}_{a}(\epsilon)$. The parameters ϵ_a are the on-site energies of the electronic sites of the spin dimer introduced in (1). The retarded selfenergies, that encapsulate the effect of the electrodes, were taken to be

$$\hbar\Sigma^{(+)}_{1}(\epsilon) = t_{\mathrm{L}}^2\frac{\epsilon}{2(J^2+\epsilon^2)} - \mathrm{i}t_{\mathrm{L}}^2\frac{J^2}{J^2+\epsilon^2}, \tag{A.29}$$

$$\hbar\Sigma^{(+)}_{2}(\epsilon) = t_{\mathrm{R}}^2\frac{\epsilon}{2(J^2+\epsilon^2)} - \mathrm{i}t_{\mathrm{R}}^2\frac{J^2}{J^2+\epsilon^2}, \tag{A.30}$$

with t_{L} and t_{R} being the tunneling amplitudes from site 1 to the left electrode and from site 2 to the right electrode, respectively. This simple model for $\Sigma^{(+)}_{a}(\epsilon)$ captures the basic physics where each electrode has an electron band whose energy band-width is approximately $4J$.

References

[1] Myers E B, Albert F J, Sankey J C, Bonet E, Buhrman R A and Ralph D C 2002 Thermally activated magnetic reversal induced by a spin-polarized current *Phys. Rev. Lett.* **89** 196801

[2] Kiselev S I, Sankey J C, Krivorotov I N, Emley N C, Schoelkopf R J, Buhrman R A and Ralph D C 2003 Microwave oscillations of a nanomagnet driven by a spin-polarized current *Nature* **425** 380–3
[3] Kiselev S I, Sankey J C, Krivorotov I N, Emley N C, Rinkoski M, Perez C, Buhrman R A and Ralph D C 2004 Current-induced nanomagnet dynamics for magnetic fields perpendicular to the sample plane *Phys. Rev. Lett.* **93** 036601
[4] Tsoi M, Fontana R E and Parkin S S P 2003 Magnetic domain wall motion triggered by an electric current *Appl. Phys. Lett.* **83** 2617–9
[5] Allwood D A, Xiong G, Cooke M D, Faulkner C C, Atkinson D, Vernier N and Cowburn R P 2002 *Science* **296** 2003
[6] Beach G S D, Nistor C, Knutson C, Tsoi M and Erskine J L 2005 *Nature Mater.* **4** 741
[7] Tatara G and Kohno H 2004 *Phys. Rev. Lett.* **92** 086601
[8] Allwood D A, Xiong G, Faulkner C C, Atkinson D, Petit D and Cowburn R P 2005 *Science* **309** 1688
[9] Duine R A, Núñez A S and MacDonald A H 2007 *Phys. Rev. Lett.* **98** 056605
[10] Bazaliy Y B, Jones B A and Zhang S C 1998 *Phys. Rev.* B **57** R3213
[11] Fernández-Rossier J, Braun M, Núñez A S and MacDonald A H 2004 *Phys. Rev.* B **69** 174412
[12] Vlaminck V and Bailleul M 2008 *Science* **322** 410
[13] Slonczewskii J C 1996 Excitation of spin waves by an electric current *J. Magn. Magn. Mater.* **159** L1
[14] Berger L 1996 Emission of spin waves by a magnetic multilayer traversed by a current *Phys. Rev.* B **54** 9353
[15] Núñez A S and MacDonald A H 2006 *Solid State Commun.* **139** 31
[16] Hirjibehedin C, Lutz C and Heinrich A 2006 Spin coupling in engineered atomic structures *Science* **312** 1021
[17] Hirjibehedin C F, Lin C-Y, Otte A F, Ternes M, Lutz C P, Jones B A and Heinrich A J 2007 Large magnetic anisotropy of a single atomic spin embedded in a surface molecular network *Science* **317** 1199
[18] Loth S, von Bergmann K, Ternes M, Otte A F, Lutz C P and Heinrich A J 2010 Controlling the state of quantum spins with electric currents *Nature Phys.* **6** 340
[19] Meier F, Zhou L, Wiebe J and Wiesendanger R 2008 Revealing magnetic interactions from single-atom magnetization curves *Science* **320** 82
[20] Chen X, Fu Y-S, Ji S-H, Zhang T, Cheng P, Ma X-C, Zou X-L, Duan W-H, Jia J -F and Xue Q-K 2008 Probing superexchange interaction in molecular magnets by spin-flip spectroscopy and microscopy *Phys. Rev. Lett.* **101** 197208
[21] Bogani L and Wernsdorfer W 2008 Molecular spintronics using single-molecule magnets *Nature Mater.* **7** 179
[22] Delgado F, Palacios J J and Fernández-Rossier J 2010 *Phys. Rev. Lett.* **104** 026601
[23] Nunez A S and Duine R A 2008 Effective temperature and Gilbert damping of a current-driven localized spin *Phys. Rev.* B **77** 054401
[24] Kampen N V 1981 *Stochastic Processes in Physics and Chemistry* (Amsterdam: North-Holland)
[25] Risken H 1989 *The Fokker–Planck Equation Methods of Solution and Applications* (*Springer Series in Synergetics*) (Berlin: Springer)
[26] Katsura H, Balatsky A V, Nussinov Z and Nagaosa N 2006 Voltage dependence of Landau-Lifshitz-Gilbert damping of spin in a current-driven tunnel junction *Phys. Rev.* B **73** 212501
[27] Auerbach A 1994 *Interacting Electrons and Quantum Magnetism* (New York: Springer)
[28] Negele J W and Orland H 1998 *Quantum Many-Particle Systems* (Boulder, CO: Westview Press)
[29] Blanter Y M and Büttiker M 2000 Shot noise in mesoscopic conductors *Phys. Rep.* **336** 1
[30] Rammer J 2007 *Quantum Field Theory of Non-equilibrium States* (Cambridge: Cambridge University Press)
[31] Datta S 1997 Electronic transport in mesoscopic systems *Cambridge Studies in Semiconductor Physics and Microelectronic Engineering* (Cambridge: Cambridge University Press)
[32] Zinn-Justin J 2002 *Quantum Field Theory and Critical Phenomena* (Oxford: Oxford University Press)
[33] Žitko R and Bonča J 2010 *New J. Phys.* **12** 063040
[34] Sothmann B and König J 2010 *New J. Phys.* **12** 083028
[35] Edwards D M, Federici F, Mathon J and Umerski A 2005 *Phys. Rev.* B **71** 054407